New characteristic relations in type-II Intermittency

E. del Rio*

Dpto. Fisica Aplicada. ETSI Aeronauticos. Universidad Politecnica de Madrid, 28040 Madrid, Spain.

Sergio Elaskar†

Dpto. de Aeronautica. Facultad de Ciencias Exactas, Fisicas y Naturales.

Universidad Nacional de Cordoba. Avenida Velez Sarfield, 161. 5000 Cordoba, Argentina.

(Dated: July 24, 2009)

We study analytical and numerical the reinjection probability density for type-II intermittency. We find a new one-parameter class of reinjection probability density where the classical uniform reinjection is a particular case. We derive a new duration probability densities of the laminar phase and a new characteristic relations. The analytical results are in agreement with the numerical simulations.

PACS numbers:

I. INTRODUCTION.

Intermittency is a particular form of deterministic chaos, in which transitions between different behaviors of the system occur. In a crisis-induced intermittency the transitions take place between chaotic attractors [1, 2]. In the Pomeau and Manneville intermittency transitions between laminar and chaotic phases occurs. A system is in a regular behavior until, with a small change in a parameter, it begin to show chaotic burst at irregular intervals [2]. Pomeau and Manneville introduce this intermittency concept relates to the Lorenz system [3, 4]. Intermittency has been studied in many experiments, associated to Benard convection [5], electronic circuits [6, 7] or human heart [8], for instance.

Type-II intermittency is one of the three intermitencies proposed by Pomeau and Manneville and it being in a subcritical Hopf bifurcation. The reinjection mechanism into laminar region dependent on the chaotic phase behavior, so it is a global property, and it was reported that is an important factor in the scaling relation of the laminar length [9, 11, 12]. Hence the probability density of reinjection (PRD) of the system back from chaotic burst into the laminar zone is determined by the dynamics in the chaotic region. Only in a few case it is possible to get analytically a function for PRD, let say $\phi(x)$. It is also difficult to get PRD experimentally or numerically, because the large number of data needed to cover each

*Electronic address: ezequiel.delrio@upm.es

†Electronic address: selaskar@efn.uncor.edu

interval of length Δx in the reinjection region. Because of this, different approximations have been used in literature to study the intermittency phenomenon. The most commun approximation is to consider PRD uniform and thus independent of the reinjection point [5, 10–17]. In different investigations it is assumed other rather artificial approximations and it is consider that the reinjection is in a fixed point [12, 18].

In this research we present a new one-parameter class of PRDs appearing in many maps with inttermitency and also in electronic circuits [6]. For a specific value of the parameter, the new PRDs recover the classical uniform PRD. We also derive the new scaling properties in good agreement with the numerical simulations.

We study a illustrating model

$$x_{n+1} = G(x_n) \equiv \begin{cases} F(x_n) & x_n \leq x_r \\ (F(x_n) - 1)^{\gamma} & x_n > x_r \end{cases} \qquad (1)$$

where $F(x) = (1+\epsilon)x_n + (1-\epsilon)x_n^p$, and x_r is the root of the equation $F(x_r) = 1$ (see Fig. 1). The origin $x = 0$ is always a fixed point. It is stable for $\epsilon < 0$. On the contrary, it is unstable for $\epsilon > 0$, and the iterated points x_n of a starting point x_0 closed to the origin, increases in a process driven by parameters ϵ and p. When x_n becomes larger than x_r, a chaotic burst occurs that will be interrutted when x_n is again mapped into the laminar region.

For $\gamma = 1$ the map (1) can be write as $x_{n+1} = (F(x_n)$ mod 1) and if in addition $p = 2$ the map is the same that used by Manneville in his pioneer paper [17]. The case

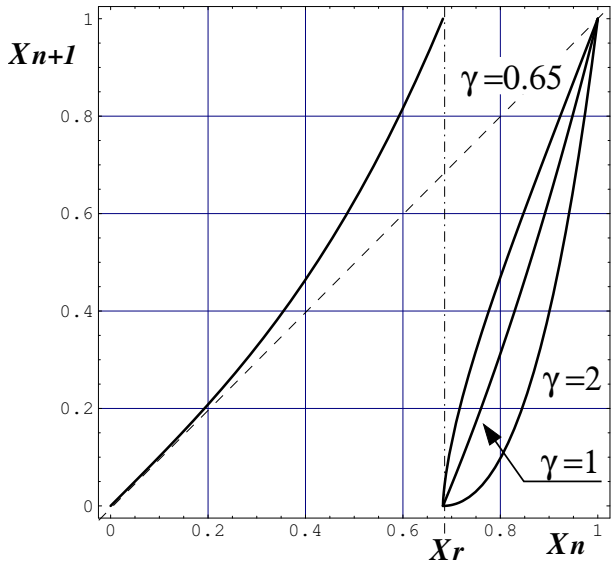

FIG. 1: Map of Eq. (1) with $p = 3$ and $\epsilon = 10^{-3}$. We have used three differed values of γ as it is indicated.

$p = 3$ corresponds with the local Poincare map of type-II intermittency for points closed to $x = 0$. Note that ϵ and p modified the duration of the called laminar phase where the dynamics of the system look like periodic and x_n is less than some value, let said c. The mathematical function for PRD, let say $\phi(x)$, will strongly depend on parameter γ, that determines the curvature of the map in region around of x_r with $x > x_r$. Only points in that region will be mapped inside of the laminar region. Note that when γ increases, also increases the number of points that will be mapped around the unstable fixed point $x = 0$.

Section II is devoted to present a methot to determine the PRD with low noise. The new scaling properties are derived in Section II. Finally in Section III we provide the conclusions and we present a similar case of reinjencion that can be solve analytically and them can be help us

to get an analytical estimation of the PRD.

II. REINJECTION PROBABILITY DISTRIBUTION

It is clear that PRD is driven by chaotic behavior of the system, and then it depends on the particular systems. In general it is very difficult to get analytically $\phi(x)$, howewer, for the map (1) we can used a simple analysis to guess the behavior of $\phi(x)$ near $x = 0$, as the parameter γ changes. To do this, note that all point failing closed to the point $x = 0$, are coming from the point closed to $x = x_r$, so $\phi(x)$ is connected with $\rho(x')$ where ρ is the invariant density for the map (1), and x' is one iteration back, that is $x' = G_2^{-1}(x)$, where $G_2^{-1}(x)$ is the inverse function of $G(x)$ but considering only the definition for $x > x_r$. We need also to rescale $\rho(x')$ take into account the slope of the function G for points closed to x_r and laying in the right side of x_r. Hence we get for points closed to $x = 0$

$$\phi(x) = \rho(x') \frac{C}{\left.\frac{\mathrm{d}G(\tau)}{\mathrm{d}\tau}\right|_{\tau=x'}} \tag{2}$$

where C is a normalization constant such that $\int_0^c \phi(\tau)d\tau = 1$.

Note that in Eq. (2), the slope $\lim_{\tau\to x_r^+} \left.\frac{\mathrm{d}G(\tau)}{\mathrm{d}\tau}\right|_{\tau=x'}$ is zero for values of γ bigger than 1 and we have $\lim_{\tau\to x_r^+} \left.\frac{\mathrm{d}G(\tau)}{\mathrm{d}\tau}\right|_{\tau=x'} = \infty$ if $\gamma < 1$ (see Fig. 1). Hence, we expect that for $\gamma < 1$ the PRD vanished near $x = 0$ and on the other hand, if $\gamma > 1$ we expect $\lim_{x\to 0^+} \phi(x) = \infty$.

In this paper we do not measurement $\phi(x)$ directly from the numerical data. Instead of this we used the function $M(x)$ defined as following

$$M(x) = \frac{\int_0^x \tau\phi(\tau)d\tau}{\int_0^x \phi(\tau)d\tau}. \tag{3}$$

Note that for uniform reinjection we get $M(x) = mx$ with $m = 1/2$.

The function (3) is very similar to the function used in [6] to determined the reinjection probability distribution in a case of type-III intermittency in a electronic circuit. In those case, experimental data indicates $M(x) \approx mx$, with m bigger than $1/2$ so $\phi(x)$ was not uniform.

We have numerically evaluate the function $M(x)$ in a broad class of maps obtaining, in good approximation, the lineal form $M(x) = mx$.

Figure (2) shows numerical evaluations of $M(x)$ for the map (1) using different values of parameter γ together with the corresponding best fit straight line. Note that the slope m can be bigger or less than the $1/2$ but always we find $|m| < 1$.

According with previous results, we assume that $M(x) = mx$, then the reinjection probability density read [6]

$$\phi(x) = bx^\alpha, \quad \text{with} \quad \alpha = -\frac{1-2m}{1-m} \tag{4}$$

where b is determined by the normalization condition

$$\int_0^c bx^\alpha dx = 1 \tag{5}$$

Assuming $\alpha > -1$, or equivalent $0 < m < 1$, the integral converge and we get

$$b = \frac{\alpha+1}{c^{\alpha+1}} \tag{6}$$

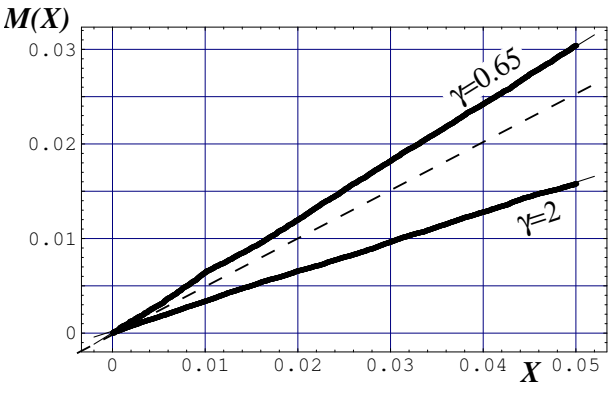

FIG. 2: Function $M(x)$ for the map (1) with $p = 3$. Points correspond to numerical evaluation of $M(x)$ and continuous lines show the cooresponding lineal fit. The dashed line slope is 0.5 and it corresponds to a uniform reinjection. In the upper line $\gamma = 2$ and $\epsilon = 10^{-3}$ whereas for the lower case $\gamma = 0.65$ and $\epsilon = 10^{-4}$. Numerical evaluation of m yields $m = 0.61$ for upper line and $m = 0.32$ for lower line. The laminar interval is $(0, c)$, with $c = 0.05$

so in the linear approximation $M(x) = mx$, the density $\phi(x)$ is determined only by the parameter m, easier to measure that the complete function $\phi(x)$.

Note that according to Eq. (4) the behavior of $\phi(x)$ near $x = 0$ can be very different from the flat line (uniform reinjection). For instance we have $\lim_{x\to 0} \phi(x) = \infty$ when m is in the interval $0 < m < 1/2$, whereas $\lim_{x\to 0} \phi(x) = 0$ when m lies in $1/2 < m < 1$. According with the previous argument from Eq. (2) we expect for $\gamma > 1$ values of m in the interval $0 < m < 1/2$ and for $\gamma < 1$ values in the interval $1/2 < m < 1$. This is in agreement that with we find numerically. For instance, in Fig. 2 we used the values $\gamma = 0.65$ and $\gamma = 2$ we obtain $m = 0.61$ and $m = 0.32$ respectively. The value of m determines, by means of eq,(4-5), the PRD function, as it is showed in figure (3). In this figure it is plotted the numerical reinjection density probabilities together with the functions $\phi(x)$ for two values of γ used in Fig. 2. Note that we do not fit the numerical data plotted in Fig. 3 but we just plot the equation (4) using the value of m calculated to plot continuous lines in Fig. 2. Note that

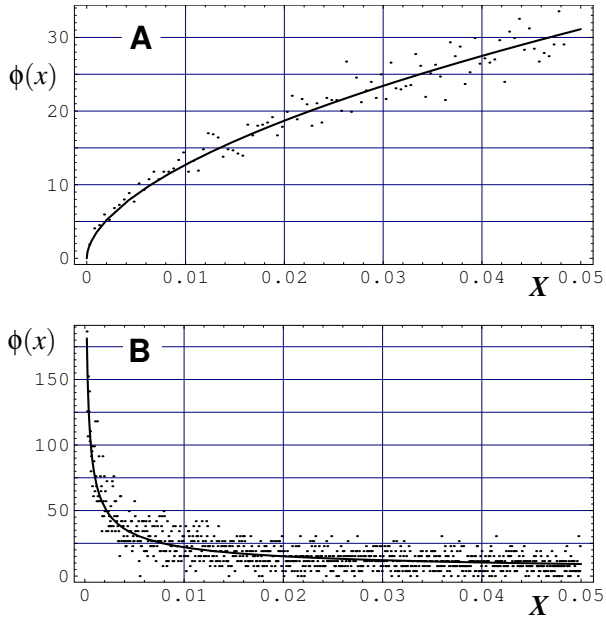

FIG. 3: Reinjection probability density for map (1) using the same parameters that in Fig. 2. Figure A and B correspond to the upper and lower cases of Fig. 2 respectively. Dots indicate numerical evaluations and continuous lines show the Eq. (4) with the value of m using to plot continuous line in Fig. 2.

the expression (4) filters the usual noise of the numerical data, hence it get better description of the numerical reinjection density. The same will happen for the legnth probability density as will be show below.

The value of m determines the value of exponent α in the reinjection function (4), hence it also drives the

characteristic relation for the average laminar length, as will study in next section.

III. CHARACTERISTIC RELATIONS

In the laminar region we can approximate the difference equation (1) by the differential equation

$$\frac{dx}{dt} = \epsilon x + (1-\epsilon)x^p \tag{7}$$

so the interactions in the laminar region, depending on the reinjection point x is given by

$$l(x,c) = \int_x^c \frac{d\tau}{a\tau^p + \epsilon\tau} \tag{8}$$

where we use the notation $a = 1-\epsilon$. After integration it yields

$$l(x,c) = \frac{1}{\epsilon}\left[\ln\left(\frac{c}{x}\right) - \frac{1}{p-1}\ln\left(\frac{ac^{(p-1)}+\epsilon}{ax^{(p-1)}+\epsilon}\right)\right]. \tag{9}$$

Note that Eq. (9) refer to a local behavior of the map in the laminar region and it determines the length of laminar period, however, the length statistic of the laminar phases is also affected by the density $\phi(x)$, which is a global propertie. The probability of finding a laminar phase of length between l and $l+dl$ is $dl\phi_l(l)$, where the $\phi_l(l)$ is duration probability density of the laminar phase. The density $\phi_l(l)$ is related with $\phi(l,c)$ by $\phi_l(l,c) = \phi(X(l,c))\left|\frac{dX(l)}{dl}\right|$, where the function $X(l,c)$ is the inverse function of $l(x,c)$. Hence, by using eqs.(4-9) and after some algebraic manipulation we get the duration probability density of the laminar phase

$$\begin{aligned}\phi_l(l,c) = \quad & b\left(\frac{\epsilon}{\left(a+\frac{\epsilon}{c^{(p-1)}}\right)e^{(p-1)\epsilon l} - a}\right)^{\frac{p+\alpha}{p-1}} \\ & \times\left(a+\frac{\epsilon}{c^{(p-1)}}\right)e^{(p-1)\epsilon l}\end{aligned} \tag{10}$$

which depends on the global parameter α determined by the slope m of the linear function $M(x)$. Figure 4 shows the analytical expression (10) using the same value of m of the upper and lower lines of Fig. 2. Also it is plotted the corresponding numerical evaluations of ϕ_l.

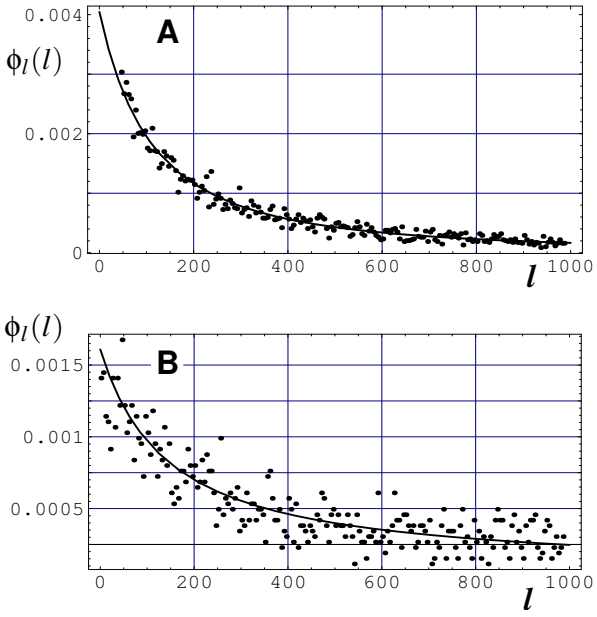

FIG. 4: Function ϕ_l for the map (1). Two different evaluations: Numerical (dots) and analytical using Eq. (10) (continuous line). The paremeters for **A** and **B** are the same that the upper and lower line of Fig. 2 respectively.

Now we consider the average laminar length $\bar{l}$ given by

$$\bar{l} = \int_0^c l(x,c)\phi(x)dx. \tag{11}$$

Then, from eqs.(4-9) and take into account Eq. (8) we get

$$\bar{l} = \lim_{x\to 0}\frac{b}{\alpha+1}l(x,c)x^{\alpha+1}\Big|_x^c + \frac{b}{\alpha+1}\int_0^c \frac{x^\alpha}{\epsilon + ax^{(p-1)}}dx \tag{12}$$

If $-1 < \alpha$, the limit in Eq. (12) is zero and the second

term can by written as

$$\bar{l} = \frac{1}{ac^{\alpha+1}} \left(\frac{a}{\epsilon}\right)^{\frac{p-\alpha-2}{p-1}} \times \left(\int_0^\infty \frac{y^\alpha}{1+y^{(p-1)}} dy - \int_{c_y}^\infty \frac{y^\alpha}{1+y^{(p-1)}} dy \right) \quad (13)$$

where $y = (a/\epsilon)^{1/(p-1)}x$ and $c_y = (a/\epsilon)^{1/(p-1)}c$. The second integral goes to zero as ϵ goes to zero, whereas the first one, converges in the parameter region $-1 < \alpha < p-2$ or equivalent $0 < m < \frac{p-1}{p}$, so we get for small values of ϵ

$$\bar{l} \approx \frac{1}{ac^{\alpha+1}} \left(\frac{a}{\epsilon}\right)^{\frac{p-\alpha-2}{p-1}} \frac{\pi}{p-1} \sin^{-1}\left(\frac{\pi(1+\alpha)}{p-1}\right) \quad (14)$$

Assuming that α remains constant as ϵ changes, the characteristic relation yields

$$\bar{l} \propto \epsilon^\beta \quad (15)$$

where the critical exponent β is given by

$$\beta = \frac{\alpha+2-p}{p-1} = \frac{1+p(m-1)}{(p-1)(1-m)} \quad (16)$$

Note that β depends on both, the behavior of the local map around the origin (parameter p), and on the global dynamics of reinjection (parameter m).

We expect that m weakly depend on parameters ϵ and p, hence for several values of γ we evaluate $\bar{l}$ as the values of ϵ change. The results are show in figure (5) for different values of γ and p.

For each point in Fig. 5 is evaluated the parameter m using Eq. (3). It is finding that it is approximately independent of γ and p, that is, m can be take as a constant in each line of the figure (5), as it is showed in table (I). Hence, according to characteristic equation Eq. (15), the

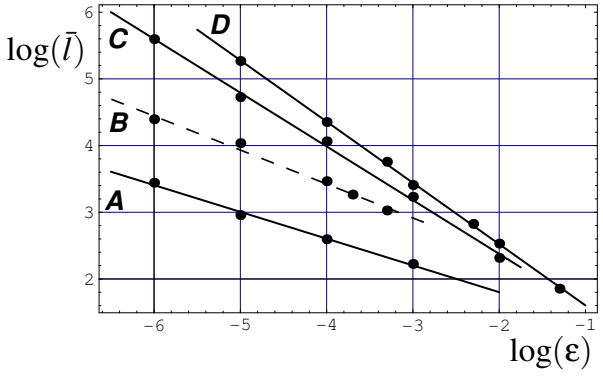

FIG. 5: Characteristic relation for different values of the parameter γ in the map (1). Dots show numerical data and lines show the best fit straight. For lines B,C and D $P = 3$ and the values of γ are 1, 2 and 3 for case A, B and C respectively. The value of parameters for line A are $P = 2$ and $\gamma = 1.5$.

TABLE I: Parameter γ and p using in each line of figure (5) and the approximate value of m associated to each line together the values of α getting for Eq. (4). Also appear the corresponding value of the exponent of Eq. (16), the numerical slope of the lines of Fig. 5 and the relative error between both.

	B	A	C	D
p	3	2	3	3
γ	1	1.5	2	3
m	0.49	0.38	0.32	0.22
α from Eq. (4)	−0.04	−0.39	−0.52	−0.72
β	−0.51	−0.39	−0.77	−0.86
Numerical slope	−0.51	−0.40	−0.80	−0.92
Relative error	$> 1\%$	3%	4%	7%

expected slope for each lines is β. Note that the slopes can be also evaluated by fitting the numerical data of the Fig. 5. The results of both methods are very closed as

appear in table (I) with the corresponding relative error. Note also that the error between analytical and numerical evaluations increases as the exponent γ increases. This effect can be due to a small nonlinearity observed in the function $M(x)$ as γ goes away from unity.

The particular value $\gamma = 1$ produces uniform reinjection in both case $p = 3$ and $p = 2$ with $m \approx 0.5$ (see dashes lines in figures 5 and 6). Hence for $p = 3$ the map exhibits the classical characteristic relation reported for type-II intermittency $\bar{l} \propto \epsilon^{\frac{1}{2}}$ which is a particular case of Eq. (16) with $p = 3$.

For $\gamma = 1$ and $p = 2$, due to $m \approx 0.5$, we are out of the range of the application of Eq. (14) and also Eq. (16). Note, however that, as $\alpha = 0$ we can evaluate the integral in Eq. (12), getting

$$\bar{l} = \frac{1}{a\,c} \ln\left(\frac{\epsilon + a\,c}{\epsilon}\right) \tag{17}$$

so for small values of ϵ we have

$$\bar{l} \approx \frac{1}{c} \left(\ln c - \ln \epsilon\right) \tag{18}$$

as it is showed in Fig. 6.

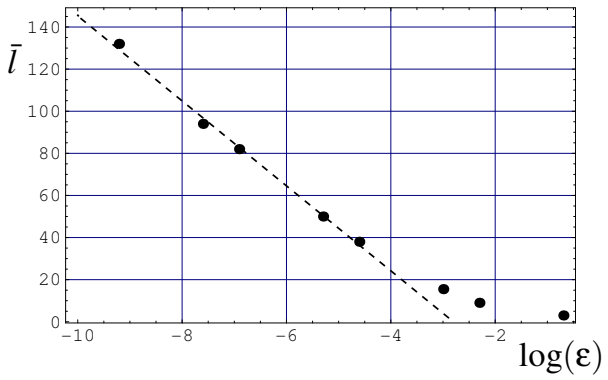

FIG. 6: Characteristic relation for the map (1) with $\gamma = 1$ and $p = 2$. Dashed line fits five points. It slope is approximately -20.2, very closed to the expected $-1/c = -20$ for uniform reinjection (see Eq. (18).

IV. DISCUSION AND CONCLUSION

Numerical iterations of maps suggests that uniform reinjection probability density is a particular case of a more general density. We present the function (3) as a tool to get the function PRD. In a number of case $M(x) \approx mx$ them we have for PRD function $\phi(x) = bx^{\alpha}$. Note that in this cases, to get a good approximation of factor m is easier than get the complete function $\phi(x)$.

It is derived a analytical expression for duration probability density of the laminar phase $\phi_l(l)$ which takes into account the local map around the unstable point and the global dynamics incorporated in the PRD formula. Also it is derived a general characteristic relation for type-II intermittency (p=3) getting for the critical exponent $-1 < \beta < 0$. All results are compared with numerical simulations finding good agreement with the analytical predictions.

As the reinjection mechanism around a unstable point is a global propertie, independent of the local instability of the map, we can study the reinjection probability density in map without intermittency. Hence, to illustrate how a nonlinear mechanism of reinjection can change the PRD from uniform reinjection ($\gamma = 1$ in Eq. (1)) to expression (4) ($\gamma \neq 1$ in Eq. (1)), we consider the well know

tent map defined as $X_{n+1} = T_1(x_n)$ where

$$T_1(x) = \begin{cases} 2x & x \leq 1/2 \\ 2 - 2x & x > 1/2 \end{cases} \tag{19}$$

Let be $H(x) = x^q$ for $q > 0$ and let be T_q defined by the composition of function

$$T_q \equiv H \circ L_1 \circ H^{-1} = \begin{cases} 2^q x & x \leq 1/2^q \\ (2 - 2x^{1/q})^q & x > 1/2^q \end{cases} \tag{20}$$

and we consider the following map $x_{n+1} = T_q(x_n)$ (see Fig. IV).

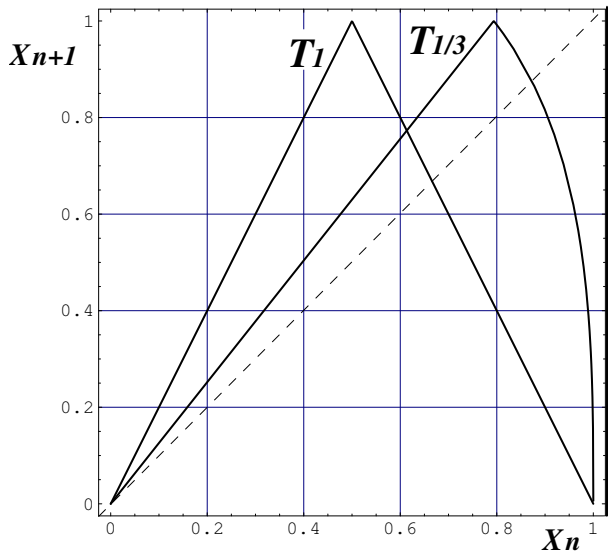

FIG. 7: Two maps T_q for $q = 1$, $1/3$. Tent map is labelled by T_1.

Note that, due to T_q is a conjugate map of the tent map, in the sense used by in [19], its invariant density $\rho_q(x)$ is related to the invariant density $\rho_1(x)$ of the tent map by[19]

$$\rho_p(x) = \rho_1(H^{-1}(x)) \left| \frac{\mathrm{d}H^{-1}}{\mathrm{d}x} \right|. \tag{21}$$

Since $\rho_1(x) = 1$ we have

$$\rho_q(x) = \frac{x^{\frac{1}{q}-1}}{q}. \tag{22}$$

then, after applied Eq. (2) for T_q we get for the PRD of the map $X_{n+1} = T_q(x_n)$ the expression $\phi_q(x) = bx^\alpha$ where

$$\alpha = 1/q - 1 \tag{23}$$

that is, Eq.(4) is exact result for $X_{n+1} = T_q(x_n)$, then we have the next exact result for $M(x)$

$$M(x) = \frac{1}{1+q} x. \tag{24}$$

In this example, the Eq. (4) appears as a natural generalization ($q \neq 1$) of the uniform reinjection ($q = 1$). It seems to be a similar mechanism for the map (1), as it is suggested from a comparison between both maps. In fact, the parameter γ in the map (1) and q in $x_{n+1} = T_q(x_n)$ play a similar roll in the sense that for $q = \gamma = 1$ we have uniform reinjection in both case. Moreover, as it is showed in Fig. 8, we can substitute in Eq.(23) q by γ to get approximated values of α for the PRD of the map (1).

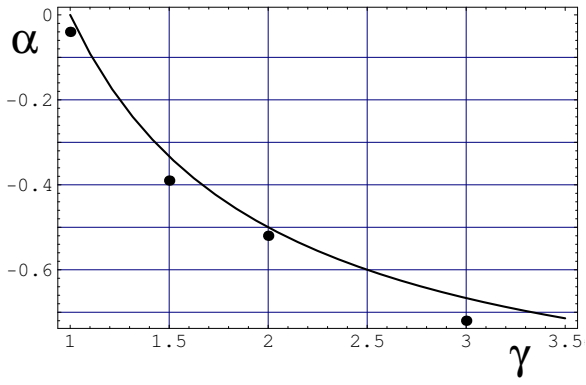

FIG. 8: Exponent α as a function of γ. Dots show the values of table (I) whereas in continuous line is plotted Eq. (23) with the identification $q = \gamma$.

Acknowledgments

This research was supported by Technical University of Madrid under grant AL09-PID-03 and by CONICET under grant PID-5269, Universidad Nacional de Cordoba and Ministerio de Ciencia y Tecnologia de Cordoba.

[1] C. Grebogi, E. Ott, F. Romeiras, J. A. Yorke, Phys. Rev. A **36**, 5365 (1987).

[2] E. Ott *Chaos in Dynamical Systems (Cambridge University Press, Cambridge, 1993*

[3] P. Manneville, and Y. Pomeau, Physical Letters A **75**, 1 (1979).

[4] Y. Pomeau, and P. Manneville, Communications in Mathematical Physics **74**, 189 (1980).

[5] Dubois, M.A. Rubio and P. Berg, Phys. Rev. Lett. **51**, 1446 (1983).

[6] E. del Rio, M. G. Velarde and A. Rodriguez-Lozano, Chaos, Solitons and Fractals **4**, 2169 (1994).

[7] S. G. Stavrinides, A. N. Miliou, Th. Laopoulos, A. N. Anagnostopoulos. International Journal of Bifurcation and Chaos **18**, 1561 (2008).

[8] J.J. Zebrowski and R. baranowski. Physica A **336** 74(2004)

[9] J.P. Crutchfield, J.D. Farmer and B.A. Huberman, Phys. Rep. **92**, 45 (1982).

[10] A.S. Pikovsky, J. Phys A **16** L109 (1983).

[11] Chil-Min Kim, O.J. Kwon, Eok-Kyun Lee, Hoyun Lee, Phys. Rev. Lett., **73**, 525 (1994).

[12] Chil-Min Kim, Geo-Su Yim Jung-Wan Ryu and Young-Jai Park, Phys. Rev. Lett. **80**, 5317 (1998).

[13] H. Schuster, and J. Wolfram, *Deterministic Chaos. An Introduction* (WILEY-VCH Verlag GmbH & Co. KGaA, Weinheim, Germany, 2005).

[14] Chil-Min Kim, Geo-Su Yim, Yeon Soo Kim, Jeong-Moog Kim and H. W. Lee Phys. Rev. E, **56**, 2573 (1997).

[15] Jin-Hang Cho, Myung-Suk Ko, Young-Jai Park and Chil-Min Kim, Phys. Rev. E, **65**, 036222 (2002).

[16] Won-Ho Kye, Sunghwan Rim and Chil-Min Kim, Phys. Rev. E, **68**, 036203 (2003).

[17] P. Manneville, Le Journal de Physique, **41**, 1235 (1980).

[18] Won-Ho Kye and Chil-Min Kim, Phys. Rev. E, **62**, 6304 (2000).

[19] Hao, Bai-lin, *Elementary Symbolic Dynamics and Chaos in Dissipatice Systems* (World Scientific Publishing Co., Singapur, 1989).